

To be submitted to
Nuclear Instr. and Meth.

COMITATO NAZIONALE PER L'ENERGIA NUCLEARE
Laboratori Nazionali di Frascati

LNF-74/36(P)
27 Giugno 1974

P. Spillantini: A HIGH-BAND NEUTRINO BEAM.

LNF-74/36(P)
27 Giugno 1974

P. Spillantini: A HIGH-BAND NEUTRINO BEAM.

In the experiments which use a wide band neutrino beam from a very high energy primary proton beam ($E_0 \gtrsim 50$ GeV) the events produced by the highest energy neutrinos ($E_\nu \gtrsim 0.2 \times E_0$) cannot be easily separated from the large number of events coming from the lower energy neutrinos. This is true especially when the kinematics of the event cannot be completely determined because the final state contains neutrinos (as in neutral current mediated events) or because some final particle cannot be recognized and measured (as is often the case in hadron deep inelastic neutrino scattering).

One way to circumvent this difficulty is to use a narrow band neutrino beam, i. e. a neutrino beam coming from a parent hadron beam selected in charge and momentum band. It is customary to make use of one or more bending magnets to select the momentum band of the parent hadron beam and some quadrupoles for its focalization^(1, 2). However this method results in a very low intensity neutrino beam even for high energy neutrinos, so that the greater cleanliness of the experiments is paid for by a loss in statistical significance. This is true also for other devices especially proposed for producing narrow band beams, such as elliptical magnetic lenses⁽³⁾ or specially shaped magnetic horns⁽⁴⁾.

2.

The way out of this difficulty is to remove the low energy hadrons ($E_h \lesssim 0.2 \times E_0$) from the parent beam, transmitting and accurately focusing all the higher energy hadrons (high-band beam).

We propose a simple device which makes use of the observation that a shaped magnetic horn of the type proposed in (4), when used for focusing a narrow band beam of momentum \bar{P}_h , strongly defocuses hadrons with $P_h \ll \bar{P}_h$, while partially focusing all hadrons with $P_h > \bar{P}_h$. This is because the quasi-parabolic profile of the horn constraints the hadrons of high momenta to remain for a longer time in the magnetic horn. The profile of the horn can be designed to focus different momenta \bar{P}_h , for different emission angles of the hadrons from the target. A circular slit at a sufficient distance from the target is then employed to select the desired hadrons (see a schematic of the layout in Fig. 1).

When a magnetic horn is used according to the design shown in Fig. 2, the exit angle of the hadron depends on its emission angle as reported in Fig. 3. The different curves correspond to different momenta of the hadron produced in a point target placed 4 m before the horn. An important feature of the system is that a ± 0.5 m displacement of the point target along the beam has a small effect only on the exit angle of the lower momentum hadrons ($P_h < 100$ GeV/c). Therefore a medium density material can be used as a target. The transmission efficiency of the system for a positive sign hadron beam produced by protons^(x) with $E_0 = 400$ GeV is reported in Fig. 4 for some different diameters of a circular slit located 30 m beyond the target.

The corresponding radial distributions of the hadrons at 400 m from the target are reported in Fig. 5. A choice of ~ 4 cm for the diameter of the slit avoids losses in the high energy hadrons band, while saving a good hadron focalization. Adopting this value for the diameter

(x) - The pion and Kaon production spectra obey the thermodynamical model; a Be target was assumed.

of the collimator, the energy spectrum of the neutrinos coming from a parent positive high-band hadron beam is shown in Fig. 6, where the spectrum of the neutrinos over a 1 m^2 detector located 830 m from the target (400 m of decay tunnel plus 430 m of shielding^(x)) is compared with the corresponding ideally focused spectrum. The attenuation of the neutrino flux with respect to the ideal one is reported in Table I for several different energy bands.

TABLE I

ΔE_ν (GeV/c)	0-50	50-100	100-150	150-200	> 200
$\frac{\text{high-band } \nu \text{ flux}}{\text{ideally focused } \nu \text{ flux}}$.12	.59	.37	.93	1

The average attenuation of the produced events is ~ 0.35 , enough to reduce substantially the analysis problems both for bubble chamber experiments and for counter experiments. In addition the flux of low-energy neutrinos is sufficient to produce a useful rate of events.

A noteworthy feature of the previously discussed high-band beam is the good collimation of the hadron beam with a very tenuous halo: with the device of Fig. 1, the maximum radius of the hadron beam ranges from 2 to ~ 40 cm along a 400 m decay tunnel (see again Fig. 5). This permits the muons coming from Kaon decays and associated with the most energetic neutrinos to emerge from the parent hadron beam, while all the other decay muons remain confined in it. This leaves open the possibility to use these muons to tag the high energy neutrino spectrum⁽⁵⁾.

(x) - This are the lenghts proposed for the West Hall ν -beam for a proton energy $E_0 = 400 \text{ GeV}$.

4.

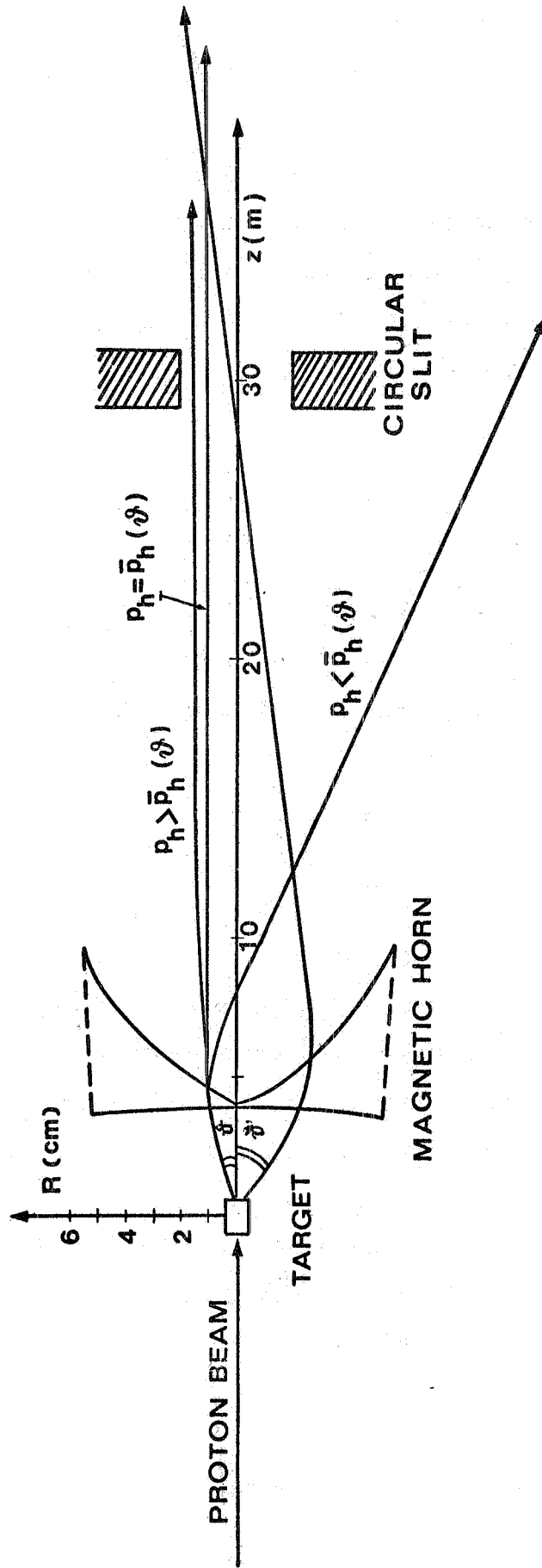


FIG. 1 - Schematic of the layout for producing a high-band neutrino beam.

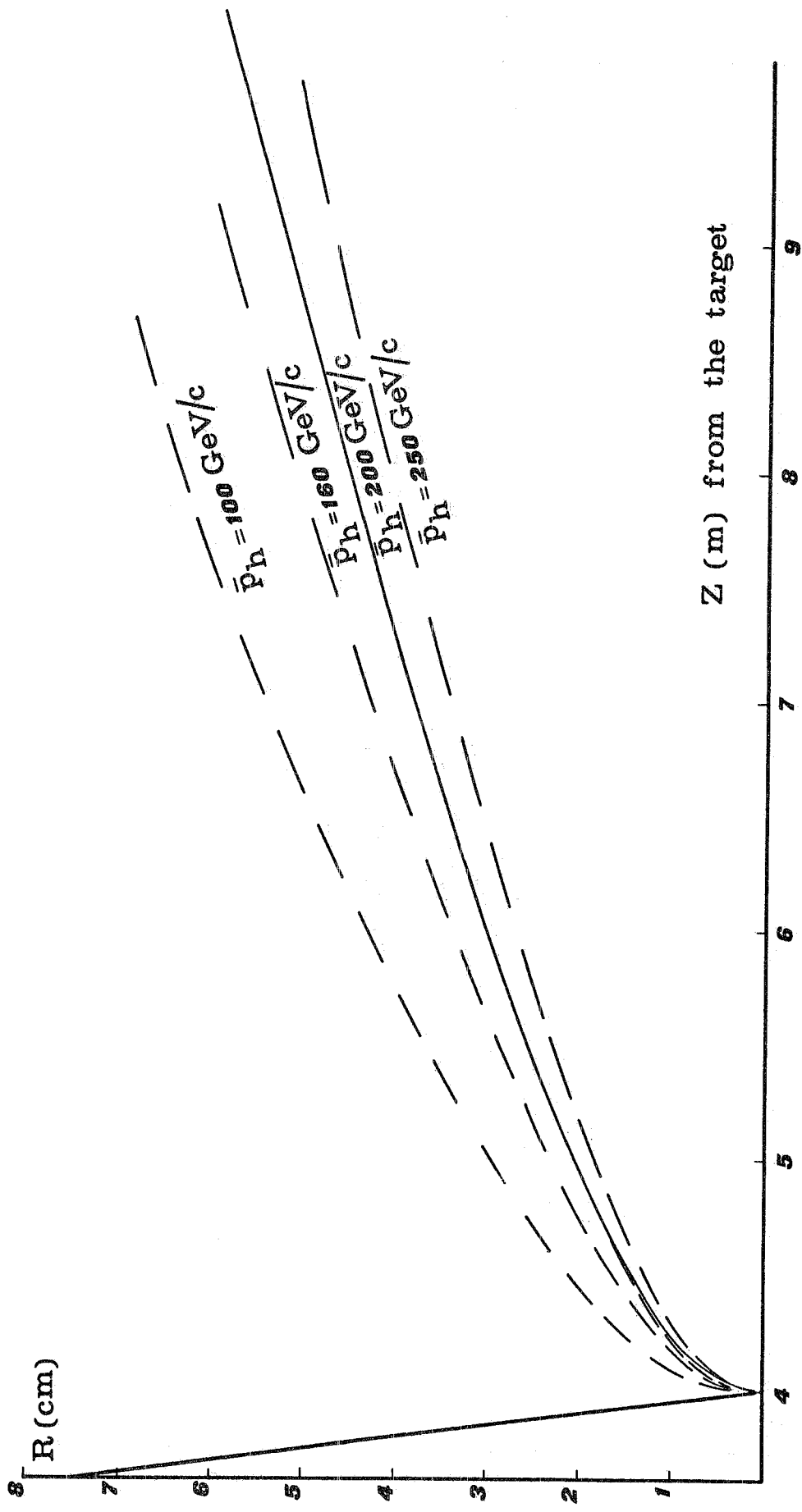


FIG. 2 - Profile of the magnetic horn to focus different momenta \bar{P}_h for different emission angles of the hadron from the target. The broken lines correspond to profiles to focus some momenta for any emission angles. The target is placed 4 m before the vertex of the horn.

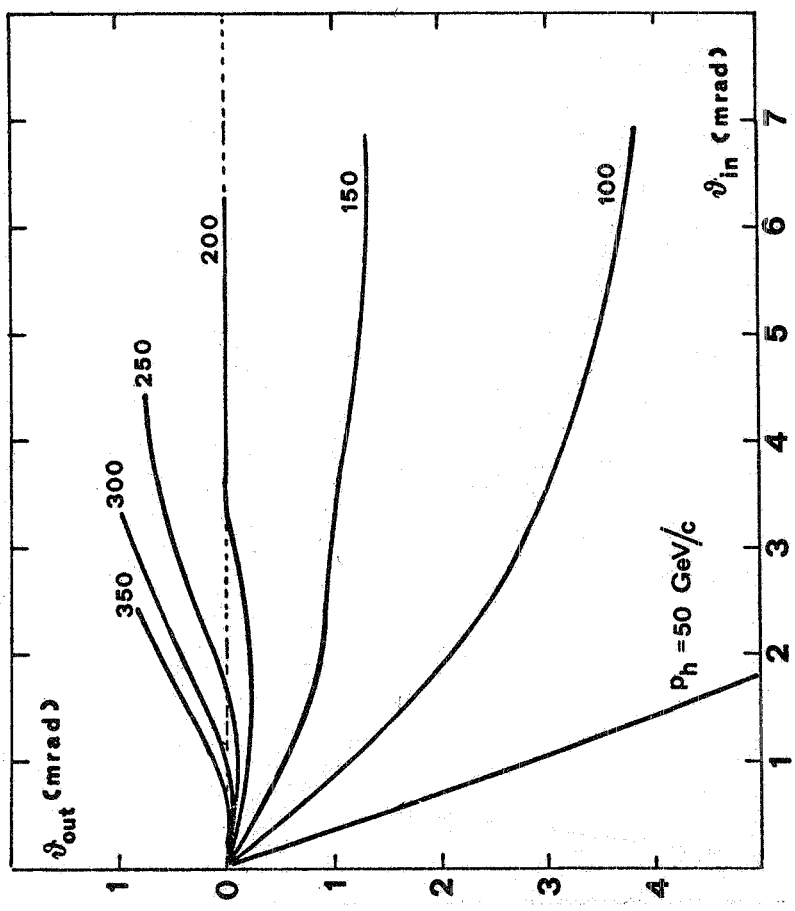


FIG. 3 - Exit angle ϑ_{OUT} from the magnetic horn of a hadron versus its emission angle ϑ_{IN} for various momenta P_h of the hadron. A point target placed 4 m before the vertex of the horn was assumed.

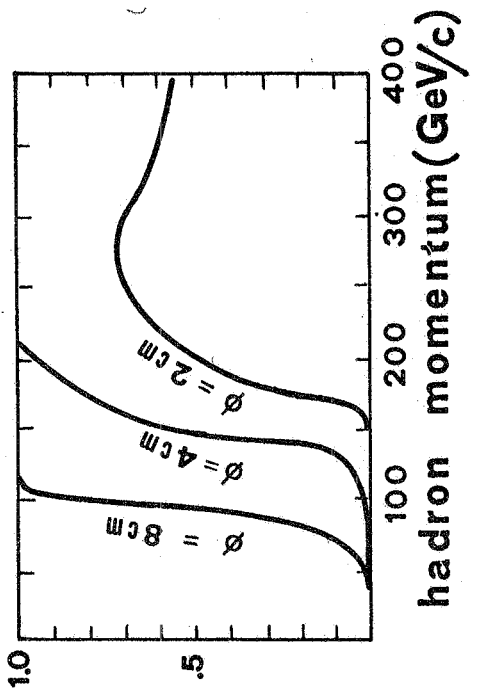


FIG. 4 - Transmission efficiency of the system drawn in Fig. 1, with the horn profile of Fig. 2 and for some different diameters of the circular slit. A primary proton energy $E_0 = 400$ GeV was assumed.

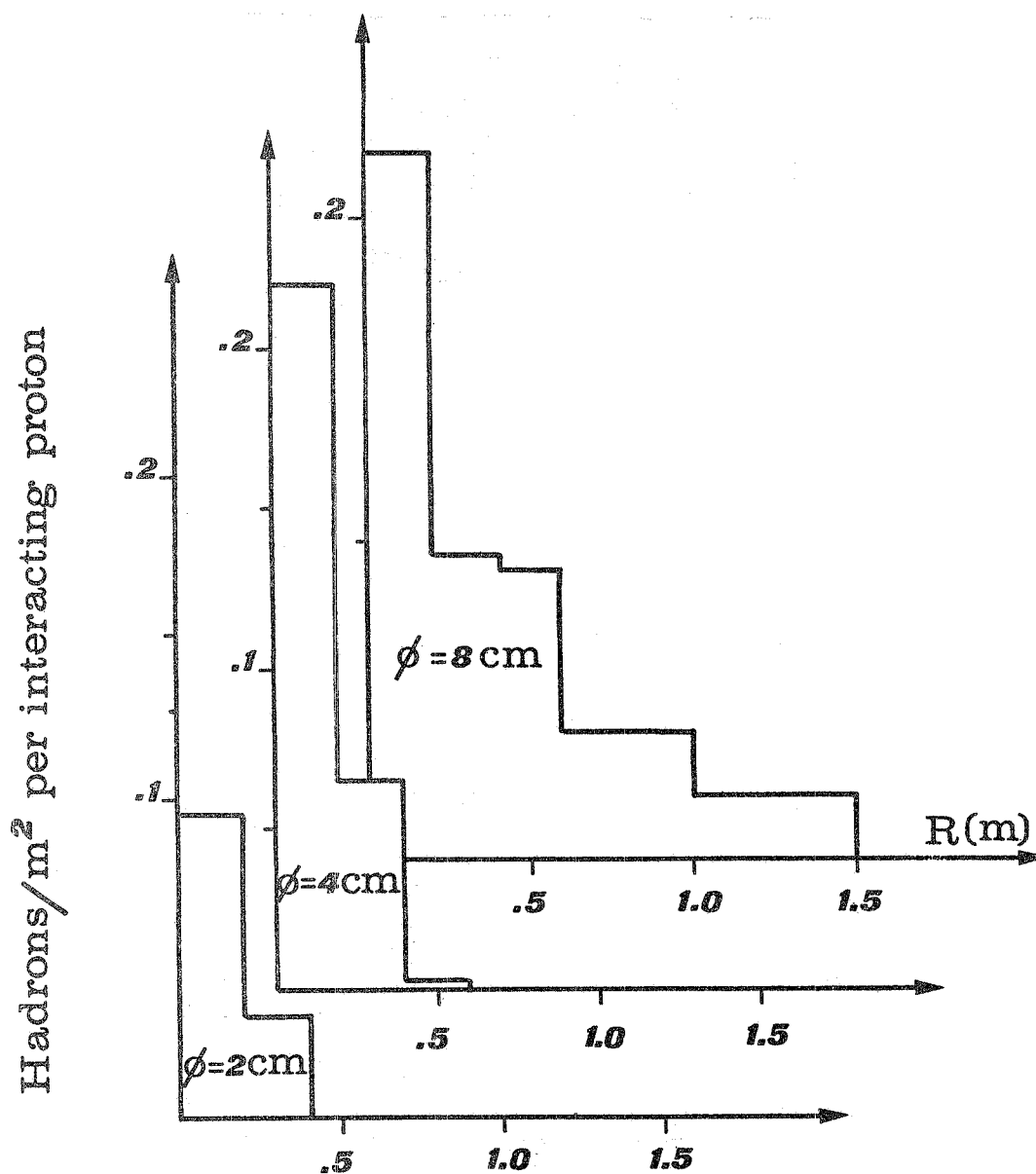


FIG. 5 - Radial distributions of the hadrons at 400 m from the target for some different diameters of the circular slit.

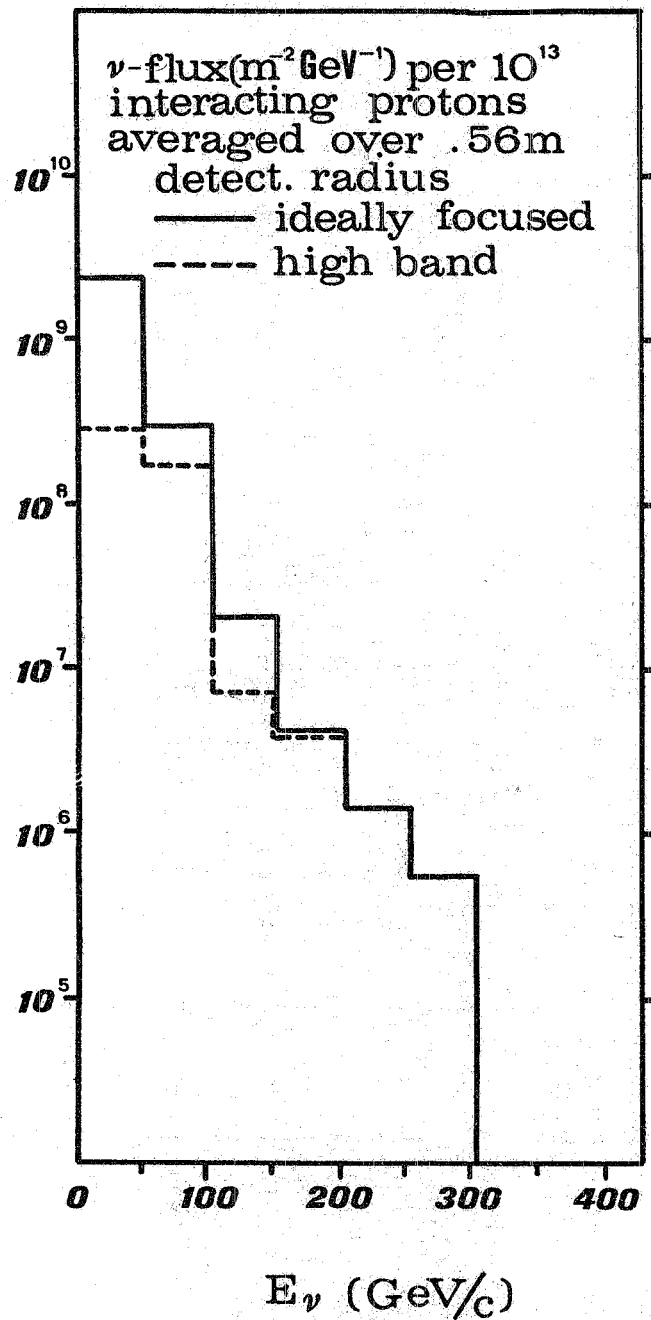


FIG. 6 - Neutrino flux ($\text{m}^{-2}\text{GeV}^{-1}$) per 10^{13} interacting protons averaged over a 1 m^2 circular detector located 830 m from the target. The full line is relative to an ideally focused beam, the broken one to the high band beam.

REFERENCES AND NOTES. -

- (1) - P. Limon, R. Stefanski, L.C. Teng, T. Yamanouchi and A. Windelborn, Nuclear Instr. and Meth. 116, 317 (1974).
- (2) - B.D. Jones and J. Lloyd, Report CERN/ECFA/WG/72-120 (1972); P. Treille and F. Vannucci CERN/ECFA/WG/72-124 (1972).
- (3) - H. Faissner, F.J. Hasert, J. Von Krook and W. Thome, Aachen Report PITHA-59 (1972) and Report CERN/ECFA/WG/72-52 (1972); V. Dohm, H. Faissner, F.J. Hasert, J. Von Krogh and W. Thome, Aachen Report PITHA-60 (1972).
- (4) - M. Brini, C. Conta, E. Fiorini and A. Pullia, Internal Milano Report (1972); C. Conta, E. Fiorini and A. Pullia, Report CERN/ECFA/WG/72-35 (1972); M. Brini, C. Conte, E. Fiorini and A. Pullia, Report CERN/ECFA/WG/72-152 (1972); M. Brini-Penso and A. Pullia, Report INFN/AE-73/10 (1973).
- (5) - P. Spillantini, Report CERN/ECFA/WG/72-168 (1972).